Journal of Molecular Catalysis A: Chemical 353–354 (2012) 80–86

Contents lists available at SciVerse ScienceDirect

Journal of Molecular Catalysis A: Chemical

journal homepage: www.elsevier.com/locate/molcata

Facile method to prepare Pd/graphene–polyaniline nanocomposite and used as new electrode material for electrochemical sensing

Zhixiang Zheng[a,b], Yongling Du[a], Qingliang Feng[a], Zaihua Wang[a], Chunming Wang[a,*]

[a] College of Chemistry and Chemical Engineering, Lanzhou University, 730000 Lanzhou, China
[b] School of Basic Medical Sciences, Ningxia Medical University, 750004 Yinchuan, China

ARTICLE INFO

Article history:
Received 29 August 2011
Received in revised form 28 October 2011
Accepted 29 October 2011
Available online 11 November 2011

Keywords:
Graphene–aniline
Graphene–polyaniline
Hydroquinone
Catechol
Charge-transfer

ABSTRACT

A new facile in situ direct synthesis method of graphene–aniline (Gr–aniline) nanocomplex by a charge-transfer self-assembly technology at organic–aqueous interface was developed in this work. The graphene nanosheets can be dissolved in aniline without any prior chemical functionalization, and then Gr–aniline is soluble in a variety of organic solvents. The graphene–polyaniline (Gr–PANI) nanocomposite was prepared by simultaneous electropolymerization of Gr–aniline, and palladium nanoparticles were loaded onto the Gr–PANI nanocomposite to be used as a new electrode material for electrochemical sensing. Hydroquinone (HQ) and catechol (CC) were used as probe molecule to evaluate the electrocatalytic activity of Pd/Gr–PANI nanocomposite. The Pd/Gr–PANI nanocomposite shows so excellent electro-catalytic activities toward the oxidation of HQ and CC isomers that the oxidation peaks of the two molecules were well and easily resolved. The excellent reproducibility, stability and selectivity of the Pd/Gr–PANI nanocomposite make it a potential candidate as electrochemical sensor for simultaneous determination of HQ and CC isomers.

1. Introduction

Graphene (Gr), a two-dimensional-monoatomic thick building block of a carbon allotrope, has emerged as a kind of new generation material of the 21st century [1], and it has drawn tremendous attention from both experimental and theoretical communities. It has been the subject of much research in recent years because of the unique electronic [2,3], thermal [4], and mechanical properties arising from its strict 2D structure [5], and its potential technical applications [6]. However, pure graphene is hydrophobic and has no appreciable solubility in most solvents [7], which limits its chemical manipulation and wide application. In order to scale up the production of graphene for technological applications, some solution properties of graphene nanosheets have also been studied aiming at their chemical modification and functionalization, such as doping [8], covalent functionalization [9], and non-covalent interactions [10]. While taking organic solvents, such as dichloromethane, chloroform, and toluene as mediums for dispersion and fabrication of graphene sheets has been rarely addressed mainly owing to their poor solubility and strong aggregation in organic solutions, there is an urgent need for a facile and efficient method to large-scale process graphene sheets in organic solvents. This expected result would further broaden the scope of applications, such as graphene-based organic and polymer composite materials or organic electronics utilizing graphene sheets as active layers [5].

On the other hand, conducting polymers (CPs) also have been extensively studied and widely applied in various organic devices [11–13]. CPs usually has to be nanostructured for improving the performance and extending the functions of the devices [12,13]. Among the CPs, polyaniline (PANI) is the earliest and potentially one of the most useful conducting polymers because of its facile synthesis, environmental stability, and simple acid/base doping/dedoping chemistry [13,14]. Nanostructured PANI can be synthesized through various chemical approaches [12,13,15].

Graphene, as a new member of carbon nanomaterial, has been applied for fabricating the composites with CPs [16,17]. The graphene–polyaniline (Gr–PANI) nanocomposite has been successfully prepared by *in* situ chemical or electrochemical polymerization, covalent or non-covalent functionalization, and self-assembly using graphene as the starting materials in most of the previous works [16–19]. But it is a pity that aggregated graphene sacrificed both large specific surface area and outstanding single-layer electric property in these processes [20,21]. For the graphene and carbon nanotubes have similar structure, the conjugated graphene sheets can be readily functionalized via non-covalent p–p, p–π stacking or covalent C–C coupling reactions through the formation of donor–acceptor complex with

* Corresponding author. Tel.: +86 9318911895; fax: +86 9318912582.
E-mail address: wangcm@lzu.edu.cn (C. Wang).

1381-1169/$ – see front matter © 2011 Elsevier B.V. All rights reserved.
doi:10.1016/j.molcata.2011.10.027

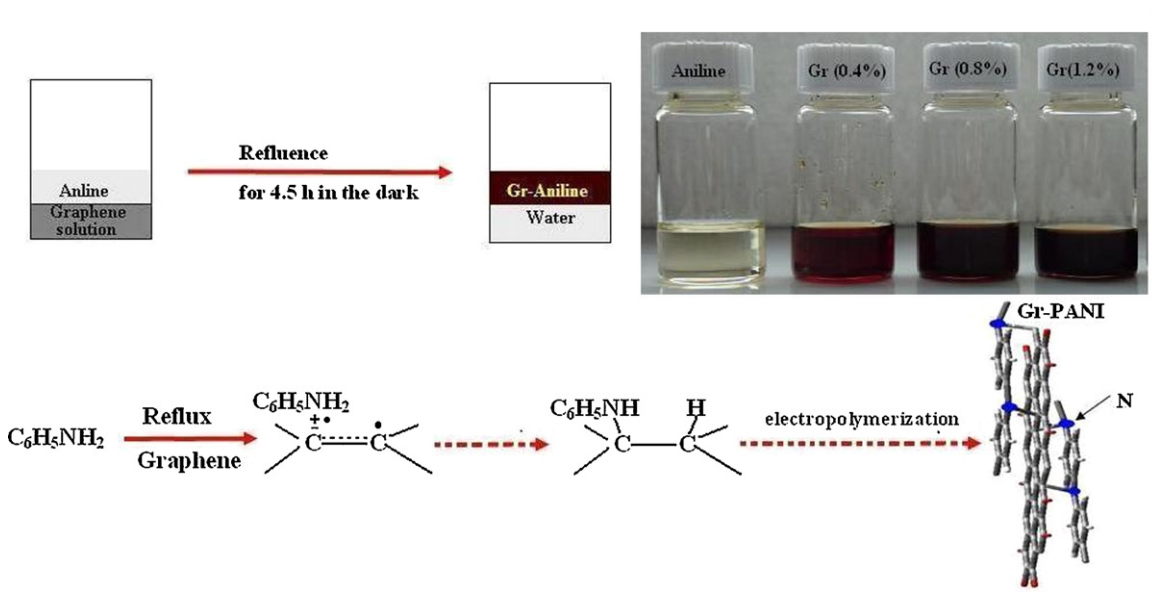

Scheme 1. The proposed reaction mechanism of a charge-transfer self-assembly process between graphene and aromatic amines, and the electropolymerization of Gr–aniline, and the schematic illustration of process for transferring graphene sheets from graphene hydrosol to aromatic amines at organic aqueous interface by refluence; the digital pictures is the different concentration (wt%) of graphene in aniline solution.

graphene plane [9]. Klaus Mullen et al. have successfully dispersed the surfactant-supported functionalization of graphene sheets in organic solvent by the phase transfer reaction [22].

In principle, for the graphene and carbon nanotubes have similar structure, graphene should be the same good electron acceptor as carbon nanotubes. While aromatic amine is a fairly good electron donor, donor type aromatic molecules can be p–π stacked on the graphene surface. And for aniline has planar aromatic structures which strongly anchor aniline onto the hydrophobic surface of graphene sheets via p–π interaction, when elevating temperatures, graphene and aniline may form a charge-transfer complex [23]. In addition, the negative charges in both molecules acting as stabilizing species to maintain a strong static repulsion force between the negatively charged graphene sheets in solution can effectively prevent the irreversible aggregation of graphene [24].

Furthermore, palladium nanostructures and its nanocomposite are drawing increasing attention in recent times due to their importance as catalytic material [25,26], hydrogen storage material [27,28], and sensors [29]. Owing to its lower cost, higher abundance, and proven electro catalytic effect on small organic molecules, it is essential to prepare Pd nanostructures containing nano-sized particles on suitable substrates to exploit the high surface area and to volume ratio and enhance catalytic activity. Therefore, the preparation of Pd nanostructures, whether solution based or coated on suitable substrates, is of considerable interest among various research groups [30–32].

In this work, for the first time, we describe a potentially and environmentally friendly method for the production of graphene–aniline (Gr–aniline) nanocomplex by a charge-transfer self-assembly technique at the organic aqueous interface of aniline and graphene colloids. The graphene–aniline nanocomplex can be readily diluted in other organic solvents (such as acetone, THF, and DMF).

Gr–PANI nanocomposites were uniformly sandwiched between layers each other by electropolymerization. And palladium nanoparticles were electrodeposited on the surface of Gr–PANI nanocomposite. The electrocatalytic activity of Pd/Gr–PANI nanocomposite was evaluated by the electro-oxidation of hydroquinone (HQ) and catechol (CC) as probe molecules in 0.5 M H_2SO_4. The voltammograms of a mixture solution of catechol and hydroquinone showed that the oxidation peaks became well resolved and separated by about 110 mV. This new type nanocomposite has high-efficiency catalytic ability and highly selective for simultaneous determination of catechol and hydroquinone isomers.

The excellent reproducibility and stability of the regular branched structures of the porous fiber Pd/Gr–PANI nanocomposite modified electrode make it suitable for simultaneous determination of hydroquinone (HQ) and catechol (CC) isomers.

2. Experimental

2.1. Preparation of graphene (Gr) colloids

The Gr colloids were prepared by the reduction of graphite oxide according to previous report [7]. Briefly, 5 mg graphite oxide, prepared from natural graphite by a modified Hummers method [33,34], was dispersed in 5 mL water to form colloids through ultrasonication of the dispersion for 30 min. Then, 5.0 μL of hydrazine solution (35 wt% in water) and 35.0 μL of ammonia solution (28 wt% in water) were added into the colloids under stirring. A few minutes later, the colloids was put in a water bath (∼95 °C) for 1 h and the graphene colloids were obtained, which was then used for the sequential reaction of a charge-transfer self-assembly technique with aniline forming hybrid Gr–aniline nanocomplex.

2.2. Preparation of Gr–PANI nanocomposite films and deposition of Pd

In a typical process, 5 mL of aniline was added to graphene hydrosol and the mixture was refluxed for 4.5 h in the dark under stirring, after which aniline is added to graphene hydrosol and the graphene is transferred to the organic phase. Dissolution transfer of graphene nanosheets into aniline can be observed by the color change of the solution after reflux for a short time. Thus, with continuous heating, the original colorless aniline solution first became brownish and then turned dark red (the digital pictures in Scheme 1 is the different concentration of graphene in aniline solution). After being cooled to room temperature, the Gr–aniline solution was obtained by separatory funnel.

The fabrication of Gr–PANI nanocomposite was completed through direct electropolymerization of Gr–aniline in 0.5 M H_2SO_4: the scan rate is 50 mV/s and the scan potential was from −0.3 to 0.9 V. The content (wt%) of graphene in Gr–aniline is 0%, 0.4%, 0.8%, 1.0%, 1.2%, 1.4%, and 1.6%, respectively (the process of electropolymerization shown in Fig. 5a). Pd nanoparticles were loaded on Gr–PANI nanocomposite through chronoamperometric technique in 0.5 M H_2SO_4 containing 1 mM $PdCl_2$ at the potential −0.30 V for 400 s.

2.3. Characterization and electrochemical measurements

The morphology of Gr–aniline, Gr–PANI and Pd/Gr–PANI was characterized on scanning electron microscopy (SEM, JSM-S4800, Japan) and transmission electron microscope (TEM, Tecnai G2 F30, FEI, USA). To verify the composition of Gr–PANI, the FTIR spectra of the products were measured. The FTIR spectra were recorded with a 4 cm^{-1} spectral resolution on Nicolet Nexus 470 spectrometer equipped with a DTGS detector by signal averaging 64 scans (Nicolet Nexus670, USA). UV–vis spectra were recorded on a lambda 35 Perkin-Elmer spectrometer.

Electrochemical measurements were carried out on a CHI 660C (USA) work station and a conventional three-electrode system. A platinum wire and a saturated calomel electrode (SCE) were used as working counter, and reference electrodes, respectively. All potentials in this work were referred to this reference electrode. The working electrode was prepared by deposition of Pd nanoparticles onto Gr–PANI nanocomposite which was electropolymerized onto glassy carbon electrode (GCE, 3 mm diameter). Prior to the fabrication, GCE was mechanically polished to mirror finished by polishing with 0.05 μm alumina paste, and cleaned thoroughly in an ultrasonic cleaner with deionized water.

2.4. Chemical reagents

Chemicals were obtained in analytical grade and used without further purification except aniline. Hydrazine solution (35 wt% in water), ammonia solution (28 wt% in water), graphite, $PdCl_2$, Na_2SO_4, H_2SO_4, HCl, $KMnO_4$, $NaNO_3$, H_2O_2, aniline, 1,4-hydroquinone (HQ) and catechol (CC) were purchased from Shanghai Chemical Co., Ltd. (Shanghai, China). Deionized water purified by the Milli-Q system (Millipore Inc., nominal resistivity 18.2 MΩ cm) was used throughout. Prior to electrochemical measurements, all the solutions were bubbled with N_2 for 15 min to remove oxygen.

3. Results and discussion

3.1. The surface morphology and optical property of graphene–aniline nanocomplex

The morphology of the graphene nanosheets dissolved in aniline was characterized by using TEM (Fig. 1). Similar to that before dissolution, the layer structured and crumpled silk veil like graphene nanosheets were observed and are in agreement with previous report [35].

The optical property of Gr–aniline nanocomplex with different Gr contents dissolved in acetone was investigated by using UV–vis spectra. Only two absorption bands were observed at 234 and 287 nm on UV–vis spectra of aniline (curve a in Fig. 2) which should be attributed to the characteristic band of aniline. The absorption band at 255–220 nm belong to B band which is the significant feature absorption band of aromatic compounds. So the absorption peak at 234 nm is the B band of aniline, and the absorption peak at 287 nm is the E2 band of aniline [23]. After graphene was added (curve b–g in Fig. 2), another two new broad bands appeared at 350 nm and 520 nm resulting from big conjugated system of graphene indicating the formation of a Gr–aniline charge-transfer complex (the formation mechanism of Gr–aniline complex is schematically depicted in Scheme 1). Additionally, the intensity of absorption at 350 nm and 520 nm increased with the content of graphene (curve b–g in Fig. 2). In very dilute solution, the peak at 350 nm and 520 nm is no longer observed. The inset of Scheme 1 is the photo of different content of graphene in aniline solution. The color of solution gradually changes to dark red with the content of graphene. These results confirmed the successful charge-transfer self-assembly of graphene sheets with aniline. The solubility of graphene in aniline is up to 1.6 wt%. This Gr–aniline nanocomplex can be readily diluted with other organic solvents such as acetone, THF, and DMF. As indicated above, we believe that a new chemical species is produced on heating graphene in aniline.

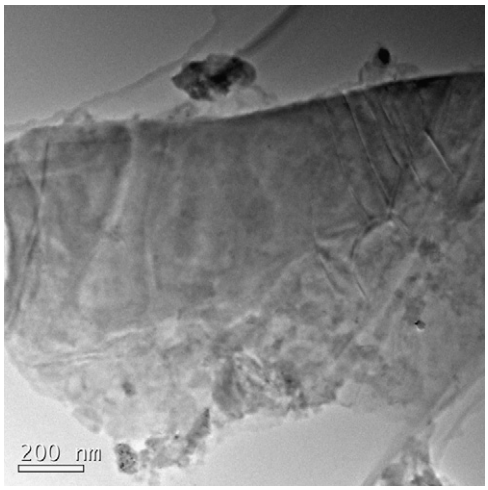

Fig. 1. TEM images of the dissolved graphene–aniline nanocomplex after evaporation of solvent.

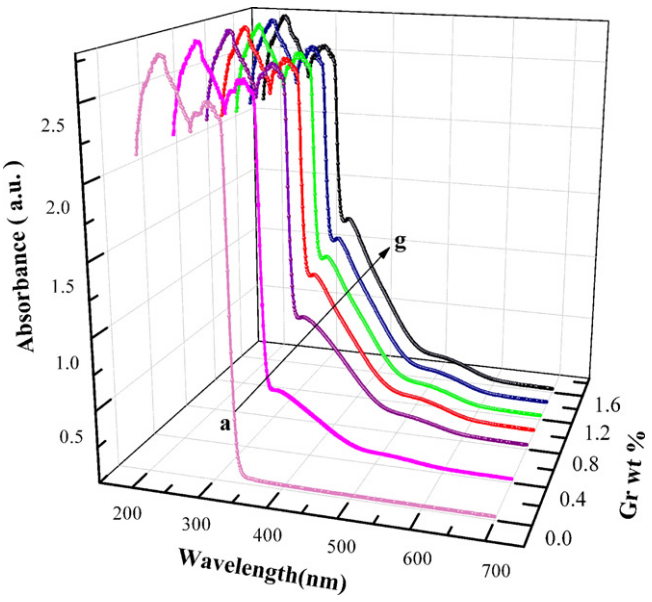

Fig. 2. UV–vis absorption spectra of Gr–aniline nanocomplex with the different content (wt%) of graphene nanosheets was dissolved in aniline solution (a–g): 0%, 0.4%, 0.8%, 1.0%, 1.2%, 1.4%, and 1.6%.

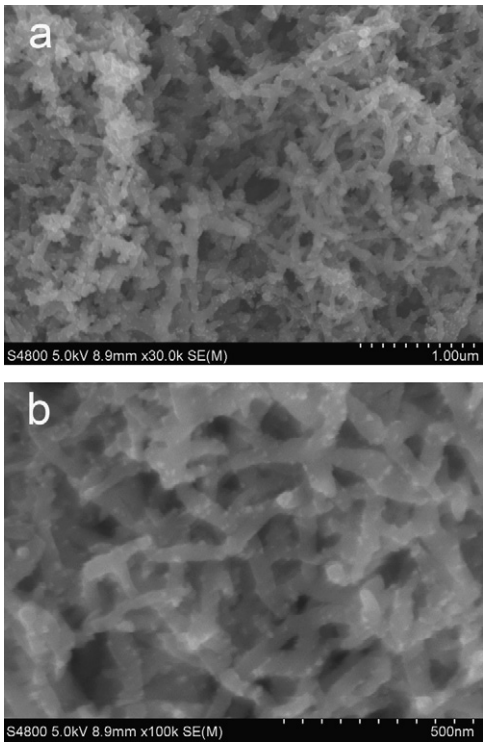

Fig. 3. Scanning electron microscopy micrographs of the regular branched structure of the porous fiber Pd/Gr–PANI nanocomposite. Scale bars: (a) 100 nm, and (b) 200 nm. The white dot is palladium nanoparticles.

3.2. The surface morphology and FTIR spectroscopy analysis of Pd/Gr–PANI nanocomposite

The SEM image of Pd/Gr–PANI nanocomposite was shown in Fig. 3. Regular branched and porous fiber structure was observed. The white spots are the Pd nanoparticles modified on the Gr–PANI nanocomposite surface. Energy dispersive spectroscopy (EDS) X-ray maps of the Pd/Gr–PANI indicated that palladium crystallites were loading on the surface of Gr–PANI nanocomposite. They were equably adsorbed on the surface of Gr–PANI nanocomposite, forming highly dispersed nanoparticles with large surface area, which may enhance the electron transport and catalytic activity of Pd/Gr–PANI nonocomposite.

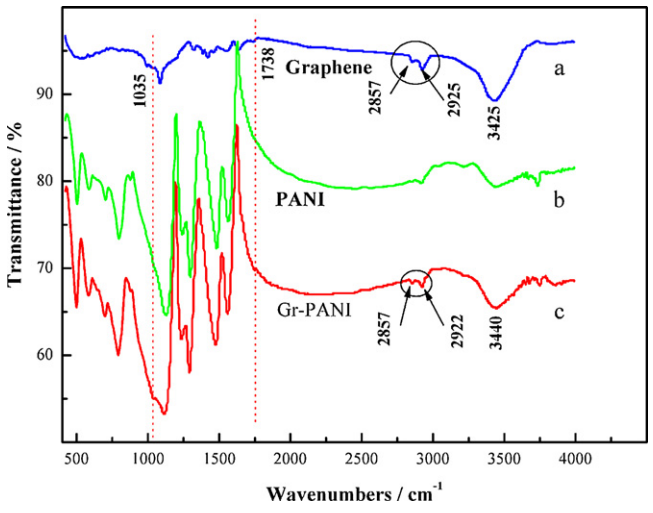

Fig. 4. FTIR spectrum of graphene, PANI and graphene–PANI nanocomposite.

Fig. 4 shows that the FTIR spectrum of pure graphene, pure PANI and Gr–PANI nanocomposite. The FTIR of graphene is in agreement with that fabricated by the hydrazine reduction method [36]. In the FTIR spectra of Gr (curve a), two absorption bands appeared at about 1639 cm^{-1} and 1738 cm^{-1} resulting from the C=O stretching mode. Another new absorption band appears at 1543 cm^{-1} which should be attributed to the skeletal vibration of the graphene sheets, as well as carboxyl C–O (1419 cm^{-1}) and alkoxy C–O (1086 cm^{-1}) groups situated at the edges of the Gr nanosheets. A broad absorption band located at 3425 cm^{-1} should be assigned to OH groups of Gr sheets (curve a). Two shoulder bands at 2875 and 2925 cm^{-1} correspond to aromatic sp^2 C–H stretching [37,38]. For PANI (curve b), the broad peak in the frequency range of 3300–3600 cm^{-1} is attributed to the N–H stretching modes of the emeraldine salt. The absorption peaks located at 1560 and 1472 cm^{-1} are ascribed to the C=C stretching deformation of the quinoid ring and benzenoid rings in the emeraldine salt [39]. The peaks at 1287 and 1120 cm^{-1} correspond to C–N stretching of the secondary aromatic amine and C=N stretching, respectively [40]. The peaks at 1130 and 790 cm^{-1} are attributed to the aromatic C–H bending in the plane and out of the plane for the 1,4-disubstitutedaromatic ring [38].

For the FTIR spectrum of the Gr–PANI nanocomposite (curve c), the C–N and C=C stretching of the quinonoid and benzenoid units appeared at 1559 cm^{-1} and 1478 cm^{-1}, respectively. The bands at 1292 and 1236 cm^{-1} are assigned to the C–N stretching of the benzenoid unit while the band at 1112 cm^{-1} is caused by the quinonoid unit of doped polyaniline. Compared with that in the case of graphene doped PANI, benzenoid and quinoid infrared peaks are slightly shifted toward the longer wavelength. The red shift of FTIR peaks can be rationalized as the change of electron density near the benzenoid and quinoid units of PANI. The broad band at 3440 cm^{-1} (curve c) can be assigned to the overlapping of the strong adsorption of the N–H stretching vibrations of PANI and OH groups of graphene. The shoulders at 2875 and 2925 cm^{-1} correspond to aromatic sp^2 C–H stretching of graphene. On the other hand, because the overlapping of the strong adsorption of PANI in this region [41,42], the precise classification is not feasible as that did for graphene. Of course, by comparison, it is still clear that the spectrum of the Gr–PANI presents the characteristic absorption of graphene nanosheets, suggesting PANI can also be successfully deposited on the graphene surface [43].

3.3. Cyclic voltammetry analysis of the Pd/Gr–PANI coated electrode

The fabrication of Gr–PANI nanocomposite was completed by using the electropolymerization method in 0.5 M H_2SO_4. The scan rate is 50 mV/s and the scan potential from −0.3 to 0.9 V. Preparation of with the content of graphene (wt%) in Gr–aniline was 0%, 0.4%, 0.8%, 1.0%, 1.2%, 1.4%, and 1.6%, respectively. The typical cyclic voltammograms of electropolymerization of Gr–aniline (Gr % = 1.2 wt%) complex in 0.5 M H_2SO_4 was shown in Fig. 5a. Three couples of typical redox peaks were observed on the CV curve. The first oxidation peak located at +0.2 V was caused by homologous oxidation of leucoemeraldine (LE) to emeraldine (EB), while the second oxidation peak at +0.48 V corresponds to the formation of the head-to-tail dimer. The last peak at +0.78 V resulted from the transform of EB to pernigraniline (PNB) [44]. It is worth noting that the peak intensity of the redox peaks increased steadily with the increase of scan circles which was indicating that the Gr–PANI deposited on the surface of electrode (GCE) continuously. This result also predicted that Gr–PANI nanocomposite films exhibit good electric conductivity and electrically active. The thickness of nanocomposite films mostly determined of the scan circle [45].

Being compared with electrochemistry polymerization of pure aniline, the peak current of peak 1 and peak 3 of every cycle

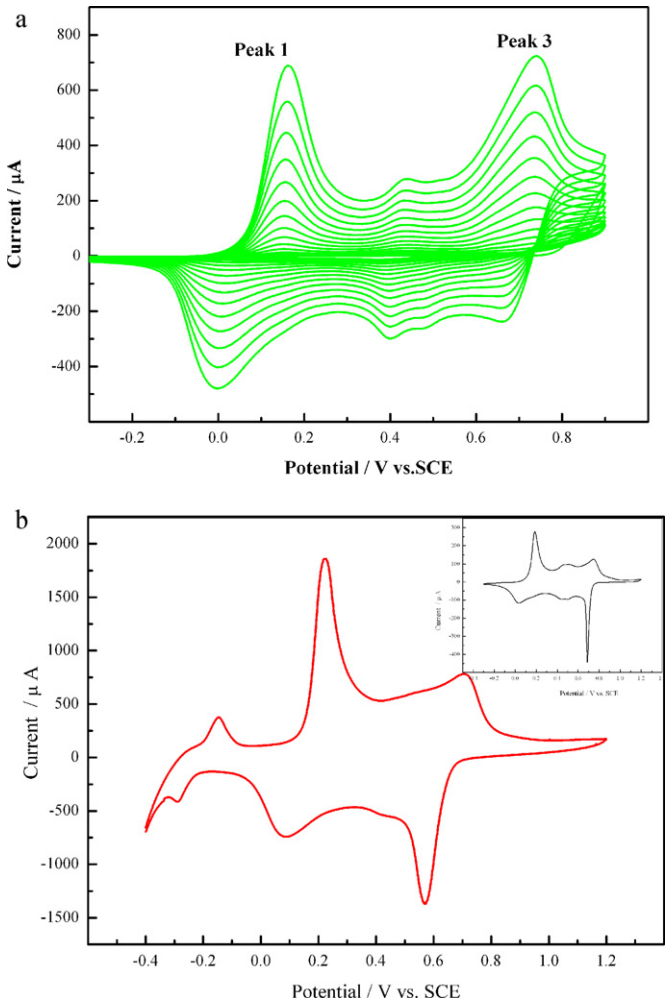

Fig. 5. The CV behavior of the growth of Gr–PANI nanocomplex films in 0.5 M H_2SO_4 + 0.1 M aniline solutions with the Gr content as 1.2 wt% (a), the CV behavior of the Pd coated Gr–PANI electrode in 0.5 M H_2SO_4 (b). Inset is the voltammogram for Gr–PANI electrode in 0.5 M H_2SO_4 (scan rate is 100 mV/s).

increased clearly, indicating that combine the graphene with aniline can improve the electron transfer rate of aniline polymerization. Additionally, the double layer capacitance at the Gr–PANI is much higher than that of PANI, which means that Gr–PANI have a much higher electrochemical active area, thus are a promising material for electrochemical applications. Pd nanoparticles were deposited on the Gr–PANI nanocomposite films in 1 mM $PdCl_2$ + 0.5 M H_2SO_4 by potentiostatic method (deposition potential is −0.50 V). Prior to the electrodeposition, the Gr–PANI films need to dip in 1 mM $PdCl_2$ + 0.5 mol/L H_2SO_4 solution for 10 min to let the metal ions can enter and completely adsorbed on the Gr–PANI films and to make regular Pd particles deposited on Gr–PANI. We have carried out cyclic voltammetry studies in acid medium to examine the affinity of hydrogen toward Pd–PANI nanofibers. Fig. 5b shows the voltammetry behavior of the Pd/Gr–PANI coated electrode in 0.5 M H_2SO_4 at a scan potential from −0.4 to 1.2 V and a scan rate at 100 mV/s. The first peak at −0.15 V corresponds to the oxidation of the adsorbed hydrogen (Had), the cathodic peak during the reverse scan is due to both absorption and adsorption of hydrogen. It is known from the literature that two well-resolved peaks for the oxidation of adsorbed and absorbed hydrogen in Pd are manifested exclusively in the case of Pd nanoparticles [46,47]. The CV results support the above observation by exhibiting the characteristic behavior of the Pd nanoparticles on the electrode surface

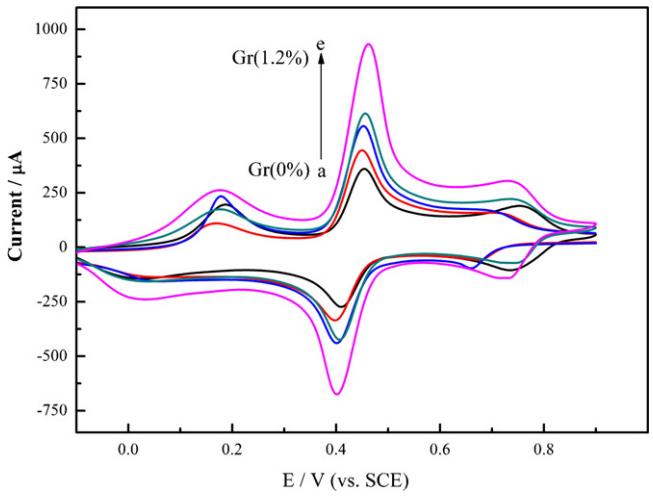

Fig. 6. The voltammograms is HQ reaction on Gr–PANI with different Gr (wt%) (Gr%: 0%, 0.4%, 0.8%, 1.0%, and 1.2%).

[37,48]. The inset is the characteristic voltammogram for Gr–PANI electrode in 0.5 M H_2SO_4. The cyclic voltammogram show two well-defined reversible redox processes characteristic of polyaniline, confirming that the polymer presents electroactivity: redox pairs at approximately 0.20 and 0.80 V, due to the oxidation lecoemeraldine/emeraldine and emeraldine/pernigraniline, respectively [49]. The Pd content of Pd/graphene–PANI nanocomposite was measured by ICP. The Pd/graphene–PANI nanocomposite was dissolved in dilute aqua Fortis for detection by ICP with a resolution of 0.01 μg/mg. The Pd content in Pd/graphene–PANI nanocomposite was 0.0430 mg cm^{-2} (RSD = 1.8%, N = 8).

3.4. Electrocatalytic activity of the Pd/Gr–PANI nanocomposite

In this work, we study the influence of graphene content in Gr–PANI nanocomposite on catalytic performance by using HQ as probe molecule. The result shows that the catalytic performance of Gr–PANI nanocomposite increased progressively with the content of graphene (the CV shown in Fig. 6).

Impedance measurements were performed for Pd/Gr–PANI by the electrochemical impedance spectroscopy (EIS). EIS is also an efficient tool for studying the interface properties of surface-modified electrodes. EIS were collected with a frequency range of 0.1 Hz–10 kHz. The EIS data were analyzed using Nyquist plots. Nyquist plots show the frequency response of the electrode/electrolyte system and are a plot of the imaginary component (Z'') of the impedance against the real component (Z'). The charge-transfer resistance (R_{ct}) at the electrode surface is equal to the semicircle diameter of EIS and can be used to describe the interface properties of the electrode. Thus, the capability of electron transfer of different electrodes was further investigated by EIS experiments. Fig. 7 indicates the results for the impedance spectrum on Pd/Gr–PANI nanocomposite: (a) electrochemistry polymerize Gr–PANI 20 cycles and electrodepositing Pd 400 s, (b) 15 cycles and electrodepositing Pd 400 s, (c) 10 cycles and electrodepositing Pd 400 s in a solution of 5.0 mM $Fe(CN)_6^{3-/4-}$ in 0.1 M KCl. Inset shows the magnified high-frequency regions. The upwards results demonstrated that the electrochemistry performance of Pd/Gr–PANI nanocomposite affected by the content of graphene in Gr–PANI.

Simultaneously, the electrocatalytic activity of Pd/Gr–PANI nanocomposite was evaluated by the electro-oxidation of the 0.01 M HQ and CC in 0.5 M H_2SO_4 and the mixture of HQ and CC in 0.5 M H_2SO_4 (see Fig. 8), respectively. The redox peaks of HQ and

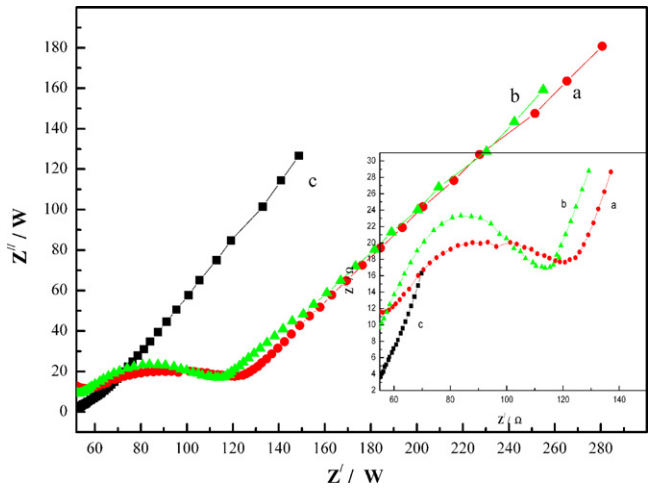

Fig. 7. Nyquist plots of different electrodes of Pd/Gr–PANI in 0.1 M KCl solution containing 5.0 mM $Fe(CN)_6^{3-/4-}$. (a) Electrodeposition PANI 20 cycles and deposition Pd of 400 s, (b) 15 cycles of 400 s, (c) 10 cycles of 400 s. Inset shows the magnified high-frequency regions.

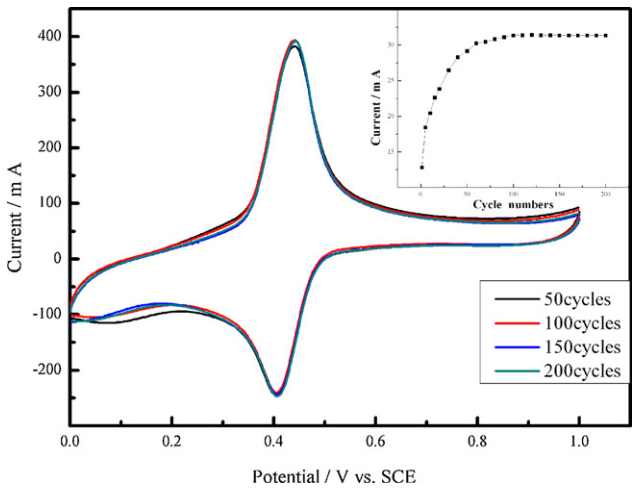

Fig. 9. The continuous CV of 50th cycle, 100th cycle, 150th cycle, 200th cycle for the electro-oxidation of 0.01 M HQ in 0.5 M H_2SO_4 under deoxygenated conditions. Inset is peak current–cycle number curve of long-term stability of Pd/Gr–PANI electrode in 0.01 M HQ + 0.5 M H_2SO_4 for continuous cyclic scan of 200 cycles (scan rate: 10 mV/s).

CC were well resolved on the Pd/Gr–PANI modified GCE and the corresponding potentials were 420 mV and 530 mV, respectively. The separation of oxidation peaks between HQ and CC was about 110 mV, in agreement with the oxidation peaks of a pure HQ and CC at this electrode, which indicate that HQ and CC can be determined respectively. The selective oxidation of HQ and CC was carried out on Pd nanoparticles modified Gr–PANI nanocomposite. It attributed to Pd inhabited some active sites of Gr–PANI and come into being space steric effect of adsorption of CC. And the Gr–PANI acts as an efficient promoter to enhance the kinetics of the electrochemical process, which is probably caused by the synergistic effect of the electrocatalytic property of Pd, graphene and PANI.

For the practical applications, the stability of Pd/Gr–PANI modified electrode was investigated using continuous CV in 0.01 M HQ + 0.5 M H_2SO_4 under deoxygenated conditions (Fig. 9).

We observed no decline in the electro-oxidation current even after 200 cycle potential scans. This behavior is attributed to the existence of numerous active sites for the adsorption HQ (the specific surface area of this modified electrode is 0.3497 cm^2). And there is no adsorption of intermediates, which can poison the catalytic surface. Another factor might be due to the doping of graphene in PANI which can improve the electrostatic forcing of the nanocomposite which is an important advantage of Pd/Gr–PANI nanocomposite ensuring high stability.

By comparing the currents of 50th and 200th scans from Fig. 9, we could know that the oxidation peak current attenuation is less than 3.0% even after 200 cycles scans. The peak current of the 200th scan is about 98% of the 50th scan. The loss of the catalytic activity after successive number of scans may result from the consumption of HQ during the CV scan. It also may be due to the diffusion process occurring between the surface of the electrode and the bulk solution. This stability of such Pd/Gr–PANI electrode can be attributed to the less poisoning of the electrode surface and the electron-rich graphene nanosheets which can effectively prevent the loss of metal catalysts. The high electrocatalytic activity and high stability indicated that the nanostructured mesoporous film can be used for further investigation and simultaneous determination for hydroquinone and catechol isomers or other isomers systems.

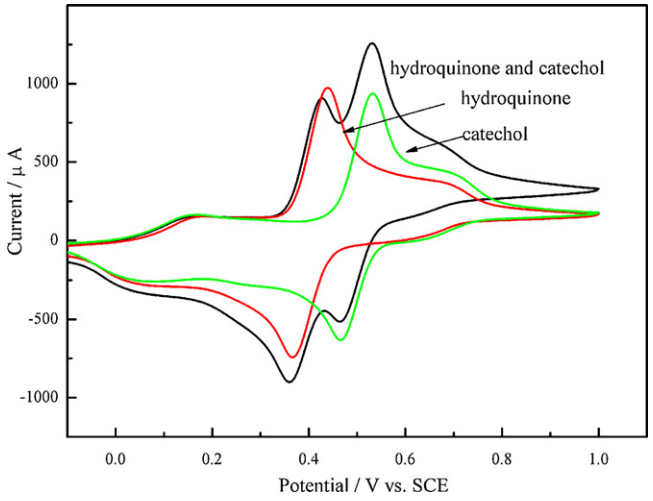

Fig. 8. Cyclic voltammograms of 0.01 M HQ (red line), 0.01 M CC (green line), intermixture containing 0.01 M HQ and CC (black line) in 0.5 M H_2SO_4 at Pd/Gr–PANI electrode (black line); scan rate is 50 mV/s. (For interpretation of the references to colour in this figure legend, the reader is referred to the web version of this article.)

4. Conclusion

A facile synthesis of graphene–aniline (Gr–aniline) nanocomplex by a charge-transfer self-assembly process is introduced. In this work, we showed that graphene nanosheets could be dissolved in aniline without any prior chemical functionalization. And then Gr–aniline is soluble in a variety of organic solvents. To our knowledge, this represents the first observation of significant dissolution of pristine graphene nanosheets in standard organic solvents. For future work involving the separation, purification, and chemical functionalization of graphene nanosheets, solubilized graphene nanosheets are a distinct advantage. For example, one can envisage graphene–aniline solutions for the formation of nanocomposite or thin films, which would solve some of the practical problems involved in making graphene nanosheets-based electronic and field emission display devices. This achievement opens up enormous opportunities to use the unique carbon nanostructure for graphene-related technological applications. Pd nanoparticles modified Gr–PANI nanocomposite can be used as new electrode material for electrochemical sensors. The Pd/Gr–PANI nanocomposite modified electrode enables enhanced electron transfer properties and improves the selectivity to the hydroquinone and catechol isomers. The excellent reproducibility and stability were

achieved on the Pd/Gr–PANI nanocomposite modified electrode indicating Pd/Gr–PANI as a promising sensing platform for selective determination of hydroquinone and catechol isomers or other cell systems.

Acknowledgements

This work was supported by National Natural Science Foundation of China (grant no. 51072073).

References

[1] K.S. Novoselov, A.K. Geim, S.V. Morozov, D. Jiang, Y. Zhang, S.V. Dubonos, I.V. Grigorieva, A.A. Firsov, Science 306 (2004) 666–669.
[2] H.B. Heersche, P. Jarillo-Herrero, J.B. Oostinga, L.M.K. Vandersypen, A.F. Morpurgo, Nature 446 (2007) 56–59.
[3] G.M. Rutter, J.N. Crain, N.P. Guisinger, T. Li, P.N. First, J.A. Stroscio, Science 317 (2007) 219–222.
[4] A.A. Balandin, S. Ghosh, W. Bao, I. Calizo, D. Teweldebrhan, F. Miao, C.N. Lau, Nano Lett. 8 (2008) 902–907.
[5] S. Stankovich, D.A. Dikin, G.H.B. Dommett, K.M. Kohlhaas, E.J. Zimney, E.A. Stach, R.D. Piner, S.T. Nguyen, R.S. Ruoff, Nature 442 (2006) 282–286.
[6] J.H. Chen, M. Ishigami, C. Jang, D.R. Hines, M.S. Fuhrer, E.D. Williams, Adv. Mater. 19 (2007) 3623–3627.
[7] D. Li, M.B. Muller, S. Gilje, R.B. Kaner, G.G. Wallace, Nat. Nanotechnol. 3 (2008) 101–105.
[8] T. Valla, J. Camacho, Z.H. Pan, A.V. Fedorov, A.C. Walters, C.A. Howard, M. Ellerby, Phys. Rev. Lett. 102 (2009) 107007–107010.
[9] Y. Xu, L. Zhao, H. Bai, W. Hong, C. Li, G. Shi, J. Am. Chem. Soc. 130 (2008) 5856–5857.
[10] B. Das, K. Eswar Prasad, U. Ramamurty, C.N.R. Rao, Nanotechnology 20 (2009) 125705–125709.
[11] C. Li, H. Bai, G.Q. Shi, Chem. Soc. Rev. 38 (2009) 2397–2409.
[12] H.D. Tran, D. Li, R.B. Kaner, Adv. Mater. 21 (2009) 1487–1499.
[13] D. Li, J.X. Huang, R.B. Kaner, Acc. Chem. Res. 42 (2009) 135–145.
[14] E.T. Kang, K.G. Neoh, K.L. Tan, Prog. Polym. Sci. 23 (1998) 277–324.
[15] S. Bhadra, D. Khastgir, N.K. Singha, J.H. Lee, Prog. Polym. Sci. 34 (2009) 783–810.
[16] J. Yan, T. Wei, B. Shao, Z. Fan, W. Qian, M. Zhang, F. Wei, Carbon 48 (2010) 487–493.
[17] D.W. Wang, F. Li, J.P. Zhao, W.C. Ren, Z.G. Chen, J. Tan, Z.S. Wu, I. Gentle, G.Q. Lu, H.M. Cheng, ACS Nano 3 (2009) 1745–1752.
[18] H. Bai, Y.X. Xu, L. Zhao, C. Li, G.Q. Shi, Chem. Commun. 166 (2009) 7–1669.
[19] P.G. Liu, K.C. Gong, Carbon 37 (1999) 706–707.
[20] D.-W. Wang, F. Li, Z.-S. Wu, W. Ren, H.-M. Cheng, Electrochem. Commun. 11 (2009) 1729–1732.
[21] X.L. Li, G.Y. Zhang, X.D. Bai, X.M. Sun, X.R. Wang, E. Wang, H.J. Dai, Nat. Nanotechnol. 3 (2008) 538–542.
[22] Y. Liang, D. Wu, X. Feng, K. Müllen, Adv. Mater 21 (2009) 1679–1683.
[23] Y. Sun, S.R. Wilson, D.I. Schuster, J. Am. Chem. Soc. 123 (2001) 5348–5349.
[24] C.H. Lu, H.H. Yang, C.L. Zhu, X. Chen, G.N. Chen, Angew. Chem. Int. Ed. 48 (2009) 4785–4787.
[25] B.J. Gallon, R.W. Kojima, R.B. Kaner, P.L. Diaconescu, Angew. Chem. Int. Ed. 46 (2007) 7251–7254.
[26] J. Hu, Y. Liu, Langmuir 21 (2005) 2121–2123.
[27] H.P. Liang, N.S. Lawrence, L.J. Wan, L. Jiang, W.G. Song, G.J.J. Timothy, J. Phys. Chem. C 112 (2008) 338–344.
[28] H. Kobayashi, M. Yamauchi, H. Kitagawa, Y. Kubota, K. Kato, M. Takata, J. Am. Chem. Soc. 130 (2008) 1828–1829.
[29] F.J. Ibanez, F.P. Zamborini, J. Am. Chem. Soc. 130 (2008) 622–633.
[30] Z. Yin, H. Zheng, D. Ma, X. Bao, J. Phys. Chem. C 113 (2009) 1001–1005.
[31] H. Meng, S. Sun, J.-P. Masse, J.-P. Dodelet, Chem. Mater. 20 (2008) 6998–7002.
[32] L.D. Burke, M.B.C. Roche, J. Electroanal. Chem. 186 (1985) 139–154.
[33] N.I. Kovtyukhova, P.J. Ollivier, B.R. Martin, T.E. Mallouk, S.A. Chizhik, E.V. Buzaneva, Chem. Mater. 11 (1999) 771–778.
[34] W.S. Hummers, R.E. Offeman, J. Am. Chem. Soc. 80 (1958), 1339-1339.
[35] J.C. Meyer, A.K. Geim, M.I. Katsnelson, K.S. Novoselov, T.J. Booth, S. Roth, Nature 446 (2007) 60–63.
[36] S. Park, J. An, I. Jung, R.D. Piner, S.J. An, X. Li, A. Velamakanni, R.S. Ruoff, Nano Lett. 9 (2009) 1593–1597.
[37] R.K. Pandey, V. Lakshminarayanan, J. Phys. Chem. C 113 (2009) 21596–21603.
[38] X.B. Yan, Z.J. Han, Y. Yang, B.K. Tay, Sens. Actuators B 123 (2007) 107–113.
[39] R. Cruz-silva, J. Romero-Garcia, J.L. Angulo-Sanchez, E. Flores-Loyola, M.H. Farias, F.F. Castillon, J.A. Diaz, Polymer 45 (2004) 4711–4717.
[40] A. Tiwaria, R. Kumar, M. Prabaharan, R.R. Pandey, P. Kumari, A. Chaturvedi, A.K. Mishra, Polym. Adv. Technol. 21 (2010) 615–620.
[41] Y.C. Si, E.T. Samulski, Nano Lett. 8 (2008) 1679–1682.
[42] S. Stankovich, R.D. Piner, S.T. Nguyen, R.S. Ruoff, Carbon 44 (2006) 3342–3347.
[43] A. Vadivel Murugan, T. Muraliganth, A. Manthiram, Chem. Mater. 21 (2009) 5004–5006.
[44] Y.-B. Shim, M.-S. Won, S.-M. Park, J. Electrochem. Soc. 137 (1990) 538–544.
[45] D.E. Stilwell, S.-M. Park, J. Electrochem. Soc. 135 (1988) 2491–2496.
[46] H.P. Liang, N.S. Lawrence, T.G.J. Jones, C.E. Banks, C. Ducati, J. Am. Chem. Soc. 129 (2007) 6068–6069.
[47] W. Pan, X. Zhang, H. Ma, J. Zhang, J. Phys. Chem. C 112 (2008) 2456–2465.
[48] X.-G. Zhang, Y. Murakami, K. Yahikozawa, Y. Takasu, Electrochim. Acta 42 (1997) 223–227.
[49] R.V. Salvatierra, M.M. Oliveira, A.J.G. Zarbin, Chem. Mater. 22 (2010) 5222–5234.